Elastic Single-ion Conducting Polymer Electrolytes: Towards a Versatile Approach for Intrinsically Stretchable Functional Polymers

Peng-Fei Cao,* [1] Bingrui Li,[2] Guang Yang,[1] Sheng Zhao,[2] Jacob Townsend,[2] Kunyue Xing,[2] Zhe Qiang,[3] Konstantinos D. Vogiatzis,[2] Alexei P. Sokolov,[1,2] Jagjit Nanda,[1] and Tomonori Saito*[1]

[1] Chemical Sciences Division, Oak Ridge National Laboratory, Oak Ridge, Tennessee 37830, United States

[2] Department of Chemistry, University of Tennessee, Knoxville, Tennessee 37996, United States

[3] School of Polymer Science and Engineering, University of Southern Mississippi, Hattiesburg, Mississippi 39406, United States

KEYWORDs: Functional polymer, Single-ion conducting, Elastic Polymer, Tunable mechanical properties

Abstract: Fabrication of stretchable functional polymeric materials usually relies on the physical adhesion between functional components and elastic polymers, while the interfacial resistance is a potential problem. Herein, a versatile approach on the molecular-level intrinsically stretchable polymer materials with defined functionality is reported. The single-ion conducting polymer electrolytes (SICPEs) were employed to demonstrate the proposed concept along with its potential application in stretchable batteries/electronics with improved energy efficiency and prolonged cell lifetime. The obtained membranes exhibit 88-252% elongation before break, and the mechanical properties are well adjustable. Galvanostatic test of the assembled cells using the obtained SICPE membrane exhibited good cycling performance with capacity retention of 81.5% after 100 cycles. The applicability of proposed molecular-level design for intrinsically stretchable polymer materials is further demonstrated in other types of stretchable functional materials including, poly(vinyl-carbazole) based semiconducting polymers and poly(ethylene glycol) based gas-separation membranes.

INTRODUCTION

Stretchable polymeric materials with specific functionalities are of great interest due to their emerging applications on stretchable devices that include rechargeable batteries/solar cells,[1-8] personal health monitors,[9] supercapacitors,[10] communication devices,[11] gas-separation membranes,[12-13] and rollup displays.[14-15] Fabrication of stretchable functional polymeric materials usually relies on the physical adhesion between functional components and elastic polymer matrix, with two main strategies: 1) utilization of stretchable polymer as interconnects between rigid island components with specific functionality; 2) embedding functional particles/molecules into elastic polymer matrices.[2, 16-17] Many efforts have been devoted to fabricate stretchable conductors by embedding electrical conductive components, including metallic nanowire/nanoparticles,[18-19] graphite/graphene,[20-21] conductive polymers,[22-23] and carbon nanotubes[24-26] into elastic polymer matrix. Stretchable sensor have been fabricated by mounting the temperature sensor,[27] strain/pressure/motion sensor,[11, 25, 28-32] electronic brain-signal monitor,[33] and multi-functional sensors[34] on the elastomeric substrates. Stretchable semiconductors are also reported to be fabricated by embedding the inorganic semiconductor (e.g. buckled silicon, GaAs ribbons and zinc oxide)[17, 35] and semiconducting polymers (e.g. poly(9,9'-dioctylfluorene-2,7-diyl-alt-benzothiadiazole, poly (thiophene))[36-39] in stretchable polymer matrix. The weak physical interaction between the plastic polymer matrix and functional units has been a technical challenge, although *in-situ* formation of elastic platform or addition of hydrogen bond has been demonstrated useful to improve the adhesion between them.[40-42] Recently, Bao and coworkers reported a highly stretchable semi-conductor by embedding the nano-confined conjugated polymer in block copolymer typed soft elastomer.[43] The nano-morphology of semi-conducting phase and compatibility between the two polymers were ensured by their comparable surface energies. Despite these significant progresses in two-part stretchable functional polymers, developing one-part stretchable functional polymers has rarely been reported, and establishing that design principle is imperative for improved mechanical/functional performance in the

stretchable devices.[17] Instead of physical adhesion, the molecular-level chemical bonding between the functional components and stretchable matrix possess the significant advantages on their compatibility.[16, 44-45] Several groups reported the synthesis of molecular-level stretchable semiconductors with conjugated polymers as rigid domain and rubbery polymer chains as the soft domain.[46-47] These approaches provide important contribution to the field, but they may lack the versatility to be generalized for applying to other types of stretchable functional materials. Moreover, elucidating the role of functional groups, polymer architectures and crosslink densities for providing desired functionalities with retained elasticity, leads to addressing one of the grand scientific challenges of controlling the mechanical property and functionality simultaneously.

Polymer electrolytes are important functional polymers for many applications including battery, super capacitor, fuel cell, actuator, ion separation and water purification.[48-50] With anions covalently immobilized on the polymer backbones to achieve cation transference number close to unity, single-ion conducting polymer electrolytes (SICPEs) are generally recognized as an advanced electrolyte system with improved energy efficiency and prolonged cell lifetime because single-ion conductivity drastically reduces electrode polarization, suppress ion concentration gradient and mitigates dendrite growth.[51-59] Among the SICPEs with different types of anions (eg. carboxylate ($-CO_2^-$), sulfonate ($-SO_3^-$), and borate ($-BR_4^-$)) interacting with Li^+, the SICPEs based on sulfonylimide anions ($-SO_2N^{(-)}SO_2-$) attracted special research attentions because its highly delocalized negative charge renders higher conductivity of Li^+ cations.[54, 60-64] The homopolymer of these sulfonylimide anions based monomers, including lithium (4-styrenesulfonyl)(trifluoromethane-sulfonyl)imide (STF-Li^+) and lithium 1-[3-(methacryloyloxy)propylsulfonyl]-1-(trifluoromethanesulfonyl) imide (MPA-Li^+), usually suffers from low conductivity at ambient temperature due to its high glass-transition temperature (T_g).[61, 63] Covalent incorporation of low-T_g polymers, mostly poly(ethylene oxide) (PEO), is a common solution to improve its conductivity, and two main strategies are commonly utilized: 1) grafting one or both ends of the high molecular-weight (MW) PEO by the polymerization of sulfonylimide-anions based monomers;[65-69] 2)

copolymerization with low MW PEO based macromers to form block or random copolymers.[63] High MW PEO based SICPEs can form free-standing polymer membranes with enhanced mechanical performance. However, the crystallinity of the PEO renders high resistance for ionic conduction when operating below its melting points (~60 °C). Although low MW PEO can address the low conductivity issues caused by crystallinity, forming a free-standing film is generally a challenge because of its low mechanical performance associated with its low T_g. In this aspect, chemical crosslinking of low MW-PEO based SICPEs should be more advantageous to address both challenges of ion conductivity and mechanical property.[64, 70]

While there are several reports on salt doped or liquid-like electrolyte (ionic liquid) nanochannel embedded stretchable ionic conducting elastomers,[71-73] achieving an elastic SICPEs, especially sulfonylimide anions based SICPEs, has not been reported yet. Herein, we report a versatile approach on the fabrication of a molecular-level stretchable functional material *via* rational polymer design. The covalent attachment of the functional side groups to a stretchable polymer network should form polymeric materials with definable functionalities and tunable mechanical properties. Just like "grape" hanging many fruits from the branches, significant amount (20-50) of functional units per side chain and numerous side chains (~30) grafting on one elastic backbone ensure functionality of the final product. The current study mainly focuses on the tailored design of high-performance stretchable SICPE, which will benefit the future stretchable batteries/electronics design considering the advantageous electrolyte performance of the SICPE based systems.[3, 8, 55, 74] This is an important step of the advancement since the fabrication of stretchable SICPE has largely been unexplored despite the numerous efforts on the solid- or gel- form SICPEs for lithium-ion or metal battery applications.[51, 63-64] Moreover, the versatility of the rational design is further demonstrated in different functional materials, including PEO based gas-separation membranes, and poly(vinyl carbazole) (PVK) based semi-conductors. This represents one of the first reports on the versatile approach for molecular-level intrinsically stretchable functional polymer materials

with defined functionalities, and the proposed strategy will be especially useful in fabricating functional materials for stretchable surfaces/devices/batteries with improved stability and long-term performance.

RESULTS AND DISCUSSION

Fabrication of stretchable single-ion conducting polymer electrolyte membranes. With relatively high stretchability, good thermal stability, chemical inertness, optical transparency and cost-effective fabrication method, polydimethylsiloxane (PDMS) is one of the most commonly used elastic polymer platforms.[13, 40] Formation of the PDMS based elastic matrix usually relies on the "curing" reaction of terminal groups, usually between Si-H groups and vinyl groups. With only two (or slightly more than two for branched PDMS) terminal groups on a typical PDMS polymer chain, it is difficult to achieve a stretchable PDMS network with high ratio of functional units (SICPEs in this case). Moreover, covalent attachment of functional units on PDMS to form di- or tri-block copolymers also affects the elastic properties of the polymers.[46-47]

Among numerous polymer architectures, grafted block copolymers are especially attractive because they provide a possibility to tune mechanical property and functionality in a relatively independent manner.[75] Herein, the PDMS having a large number of reactive amine groups (PDMS-NH_2, ~48 NH_2 per molecule with MW of 20,000 g/mol, **I** in Scheme 1(B)) were selected as the polymer backbone. The coupling reaction of the carboxylic acid terminated Reversible Addition-Fragmentation Chain Transfer Agent (RAFT-CTA-COOH, **II**) with amine groups of PDMS affords PDMS backbone containing macro RAFT-CTA (PDMS-RAFT, **III**). The comparative ^{1}H NMR spectra of PDMS-RAFT (**III**) and PDMS-NH_2 (**I**) is shown in Figure S1. Significant downfield shift of the methylene groups (CH_2, d to d' in Figure 1A) adjacent to the NH_2 manifested the formation of amide bond. Comparative signal integration of the terminal methyl groups (CH_3, j in Figure S1) in RAFT-CTA and CH_2 next to the Si allows the calculation of the degree of grafting (DG_n), i.e., 29 out of 48 amines (see Supporting Information for details). In the infra-red (IR) spectrum of PDMS-RAFT (Figure 1(B)), appearance of the

peak lying at 1645 cm^{-1} (the peak labeled with a dash line for PDMS-RAFT) corresponding to the C=O stretching of amide groups also confirmed the successful attachment of the RAFT-CTA on the PDMS backbone.

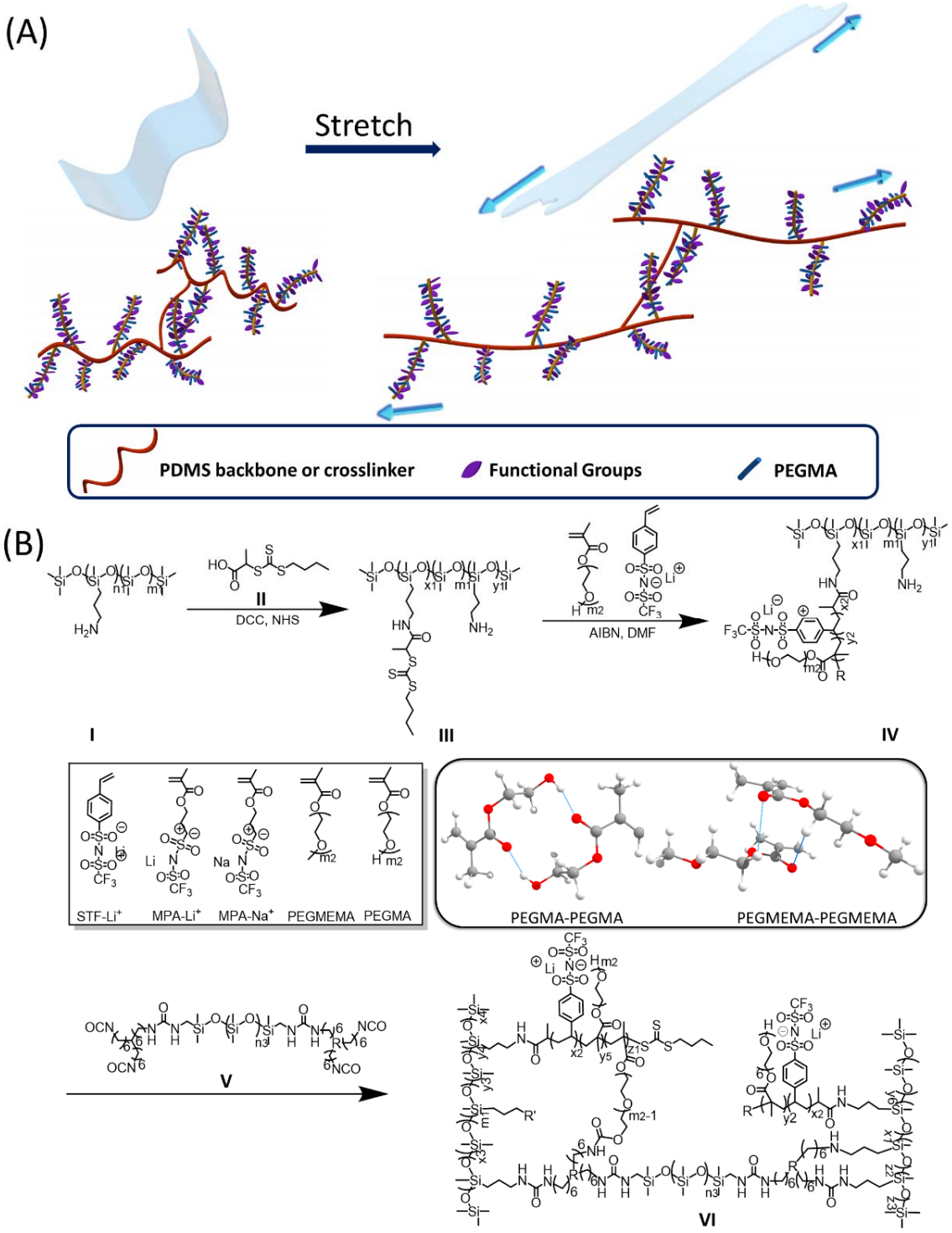

Scheme 1. (**A**) Illustration of molecular-level intrinsically stretchable functional polymers; (**B**) Synthesis of stretchable single-ion conducting polymer electrolyte, inset is the most stable PEGMA-PEGMA and PEGMEMA-PEGMEMA dimers.

With delocalized negative charge distribution, the lithium (4-styrenesulfonyl)(trifluoromethane-sulfonyl)imide (STF-Li^+) based polymer has been recognized as one of the most promising candidates of SICPE.[55] The significantly lower binding energy of Li^+ with counter ion compared with that in LiPAA also confirmed an easier ion dissociation of Li^+ from the STF-Li^+ systems (-6.3 eV *vs* -7.6 eV see Supporting Information for details). STF-Li^+ and poly(ethylene glycol) methacrylate (PEGMA) with molar ratio of 1:3 (EO:Li^+ = 18:1) were grafted from the PDMS backbone to form a grafted block copolymer PDMS-*g*-poly(STF-Li^+-*r*-PEGMA)$_{20}$ (**IV**). As illustrated in Figure 1(A), the appearance of aromatic signals (o+p, 7.0 to 8.0 ppm) suggests successful polymerization of STF-Li^+, and the significant peak lying at 3.5 ppm is attributed to the CH_2 units (s+t) in the PEO. Moreover, the IR peak lying at 1720 cm^{-1} is attributed to the C=O bond in the ester group of PEGMA. After adding PDMS crosslinker (compound **V**) and stirring at 65 $^{\circ}$C for 5 hours, the solution was poured into a Teflon dish to form an elastic polymer membrane. A freestanding, optically clear, elastic polymer membrane was obtained (See the picture in Figure S2, PDMS-poly(STF-Li^+-*r*-PEGMA)$_{20}$-PDMS$_{10}$). The EDX mapping of fluorine (F) and silicon (Si) demonstrated the sufficiently homogenous distribution of lithium-ion conducting monomer (STF-Li^+) and elastic polymer backbone (PDMS), respectively (see Figure 1(C)).

Table 1. Combined basic analysis data of stretchable SICPEs; the G' value in the table is the plateau of storage modulus, Mx is the MW between the crosslinking points; see NOMENCLATURE section for the detailed information for the sample name.

NO.	Sample	Membrane Density (g/cm^3)	G'(Pa)	Crosslink density (mol/cm^3)	Mx (g/mol)	$T_{d,5\%}$ (°C)	T_g (°C)
1	PDMS-poly(STF-Li^+)$_{20}$-PDMS$_{10}$	1.4279	NA	NA	NA	221	68.5
2	PDMS-poly(STF-Li^+-r-PEGMA)$_{20}$-PDMS$_{10}$	1.3511	1.15×10^5	3.26×10^{-5}	2.75×10^4	276	-17.5
3	PDMS-poly(STF-Li^+-r-PEGMA)$_{50}$-PDMS$_{10}$	1.4288	8.36×10^4	2.37×10^{-5}	3.99×10^4	289	-32.0
4	PDMS-poly(STF-Li^+-r-PEGMEMA)$_{20}$-PDMS$_{10}$	1.2618	NA	NA	NA	320	-35.2
5	PDMS-poly(STF-Li^+-r-PEG)$_{20}$-PDMS$_{10}$	1.2691	2.65×10^4	7.50×10^{-6}	1.12×10^5	257	-22.3
6	PDMS-poly(MPA-Li^+-r-PEGMA)$_{20}$-PDMS$_5$	1.2736	4.86×10^4	1.38×10^{-5}	6.13×10^4	288	-32.5
7	PDMS-poly(MPA-Li^+-r-PEGMA)$_{20}$-PDMS$_{10}$	1.296	8.15×10^4	2.31×10^{-5}	3.72×10^4	291	-20.1
8	PDMS-poly(MPA-Li^+-r-PEGMA)$_{20}$-PDMS$_{20}$	1.2624	2.28×10^5	6.46×10^{-5}	1.29×10^4	274	-28.7
9	PDMS-poly(MPA-Na^+-r-PEGMA)$_{20}$-PDMS$_{10}$	1.2737	1.23×10^4	3.48×10^{-6}	2.42×10^5	274	-17.4

Incorporation of PEGMA plays a critical role for improving the performance of stretchable polymer membranes: a) lower the T_g value of single-ion conducting copolymers;[61] b) enhance mechanical robustness for a free-standing polymer film. Initially, grafted copolymer PDMS-*g*-poly(STF-Li^+)$_{20}$ was synthesized by grafting poly(STF-Li^+) on the PDMS-NH_2 backbone, and elastic crosslinker (**IV**) with the same molar ratio was added to obtained polymer membrane PDMS-poly(STF-Li^+)$_{20}$-PDMS$_{10}$ (**1,** in Table 1). However, the resulting membrane is very brittle and rigid. With T_g at 68.5 °C, the polymer membrane (**1**) is in glassy state at ambient temperature, which is responsible for its mechanically rigid nature. Copolymerization with PEG will significantly lower the T_g value, where addition of PEGMA results in -17.5 °C for **2** (Table 1) as compared to 68.5 °C for **1**. Therefore, the resulting polymer membranes is in a rubbery state at room temperature. Another important role of PEGMA is its capability to provide additional reactive groups with the crosslinker (compound **V**), thus improving mechanical robustness. To verify the assumption, poly(ethylene glycol) methyl ether methacrylate (PEGMEMA), that does not possess terminal reactive hydroxyl groups, was employed to copolymerize with STF-Li^+ to form the grafted copolymer PDMS-*g*-poly(STF-Li^+-*r*-PEGMEMA)$_{20}$. Following the same procedure, polymer membrane (sample **4**, Table 1) with PEGMEMA instead was obtained. As illustrated in Figure S2, the

polymer membrane (**4**) is mechanically too weak, and it even cannot be detached from the poly(tetrafluoroethylene) (PTFE) film. From the plateau of the storage modulus (G') in the rheology spectra (Figure S4), the crosslinking density (Cx) of PDMS-poly(STF-Li^+-*r*-PEGMA)$_{20}$-$PDMS_{10}$ (**2**) was calculated to be 3.26×10^{-5} mol/cm^3. Instead of having a rubbery plateau, the G' of sample **4** tends to drop significantly at low frequency, which indicates the liquid-like property of sample **4** at high temperature range. Quantum chemical calculations also suggested the higher interaction energies (-0.7 eV *vs* -0.3 eV) and shorter hydrogen bonding (1.84 Å *vs* 2.68 Å) between PEGMA-PEGMA dimers than those of PEGMEMA-PEGMEMA dimers system (insert of Scheme 1). Higher intermolecular hydrogen bonding between the PEGMAs than that of PEGMEMAs should be another reason for higher T_g value and higher modulus of PEGMA based polymer membranes.

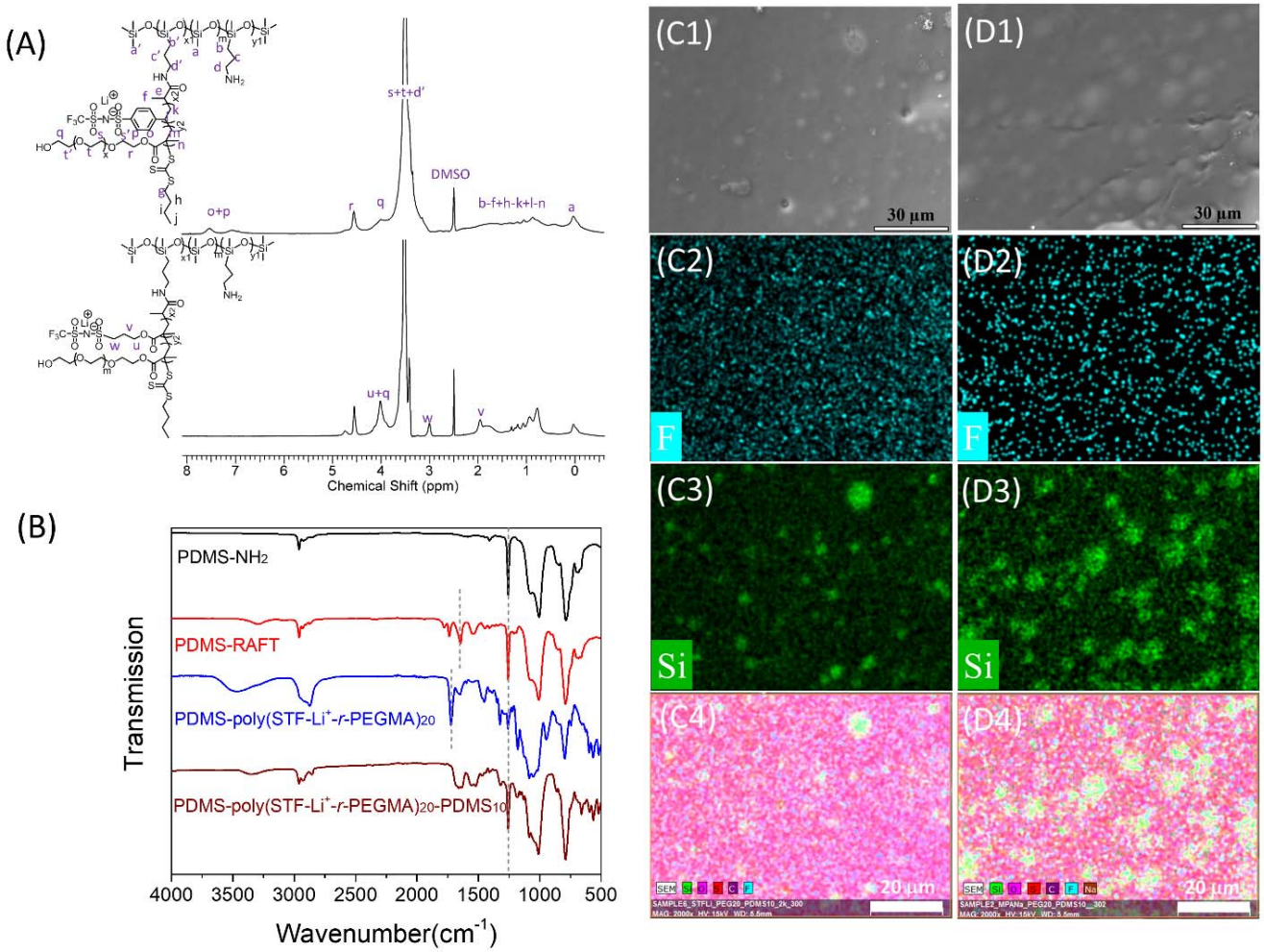

Figure 1. (A) ^{1}H NMR spectra of PDMS-poly(STF-Li^+-*r*-PEGMA)$_{20}$ (top) and PDMS-poly(MPA-Li^+-*r*-PEGMA)$_{20}$ (down); (B) FT-IR spectra of PDMS-NH_2, PDMS-RAFT, PDMS-poly(STF-Li^+-*r*-PEGMA)$_{20}$

and PDMS-poly(STF-Li^+-*r*-PEGMA)$_{20}$-$PDMS_{10}$; (C1) Scanning electron microscopy (SEM), and Energy Dispersive X-ray Spectroscopy (EDX, C2, C3 and C4) mapping of PDMS-poly(STF-Li^+-*r*-PEGMA)$_{20}$-$PDMS_{10}$; (D1) SEM and EDX (D2, D3 and D4) of PDMS-poly(MPA-Na^+-*r*-PEGMA)$_{20}$-$PDMS_{10}$; C2 and D2 shows the elementary distribution of fluoride (F), C3 and D3 shows the distribution of silicon (Si), C4 and D4 shows the combined element distribution of Si, O, S, C, F (and Na for sample **9**)

Similar to STF-Li^+, MPA-Li^+ (inset of Scheme 1(B)) is a recently developed single-ion conducting monomer. With comparatively lower T_g value due to more flexible polymer backbone, the MPA-Li^+ based single Li-ion conducting polymers are reported for improved conductivity.[63, 66] After doping with propylene carbonate (PC) as plasticizer, the gel electrolyte can even be operated at ambient temperature.[64] Following the same procedure as STF-Li^+ series (Table 1, **1**-**5**), MPA-Li^+ and MPA-Na^+ based elastic polymer membranes (Table 1, sample **7** and **9**) were also fabricated. EDX image (Figure 1(D)) demonstrated that the cation was even visible for Na^+ based polymer membranes (PDMS-poly(MPA-Na^+-*r*-PEGMA)$_{20}$-$PDMS_{10}$, sample **9**) in addition to the main elements because of the heavier nature of Na than Li. The design on sulfonylimide anion-based single sodium-ion conducting polymer electrolyte may benefit the future sodium-ion batteries. The non-crystalline nature of these polymer membranes (sample **2**, **7** and **9**, Differential Scanning Calorimetry (DSC) curves in Figure S5 and WAXS in Figure S6) should be attributed to low MW of PEG and crosslinking nature of polymer membranes. This is vital to both stretchability and Li-ion conductivity of the membranes. The presence of only one T_g in the DSC curve demonstrated the absence of significant phase separation in the obtained membranes (sample **2**,**7** and **9**). The broad peaks with Q values ranging from 0.11 to 0.20 nm^{-1} in the SAXS spectra (Figure S6) were observed. This is explained by the presence of nano-clusters rendered by the hydro-phobic interaction of RAFT-CTA. Similar phenomena have also been observed for the telechelic PDMS systems in which hydrogen bonding tails also renders the formation of nanoclusters.[76] Poly(STF-Li^+) and amorphous PEO are reported to be miscible with each other and will not result in any significant phase separation.[63, 65, 69] To eliminate the possibility that broad peaks in the SAXS spectra is due to the phase separation between PDMS matrix and PEO/poly(STP-Li^+)(poly(MPA-Li^+/Na^+) segment, SAXS analysis of the linear random

copolymer with RAFT-CTA (PEO-*r*-poly(MPA-Li^+), see Figure S7) has also been performed, and as expected, the broad peak lying at 0.19 nm^{-1} was also observed.

Mechanical performance evaluation Chemical crosslinking by isocyanate functionalized PDMS (V) will convert the liquid-like compound IV to the rubbery membranes (VI) (G' > G" over wide range of frequency and presence of rubbery plateau) at ambient temperature.[24] Physical crosslinking was also introduced to the elastic membranes due to the formation of urea (urethane) units during chemical crosslinking. Although the random copolymer PEO-*r*-poly(MPA-Li^+) is the main chemical composition (~ 80wt%), the overall mechanical property of these polymer membranes is still mainly determined by the elastic PDMS matrix, because the PDMS serves as both polymer backbones and crosslinkers. While entanglements for PEO-*r*-poly(MPA-Li^+) side chains is also possible, their contribution to overall mechanical performance should be negligible. As expected, simple hand pulling can easily extend the polymer membrane of sample **2** (Figure S8), similar to the isocyanate crosslinked PDMS membranes.[13] To quantify the mechanical property of the functional polymer membranes, rectangle-shaped polymer films with width of 5.0 mm and length of 4.0 cm have been fabricated for tensile tests (Figure 2(A)). Sample **2** (STF-Li^+ as the monomer) can be stretched up to 88% before breaks, which should satisfy the requirement of stretchable devices.[23] The elastic recovery of sample **2** was also evaluated by applying 10 cycles of 50% strain (Figure S9). As seen in the hysteresis test, sample **2** exhibited outstanding elastic performance with the residual strains as 5% when stress is back to 0 at the first cycle, and remaining stress being 95% of initial stress (108 kPa *vs* 114 kPa) when having the same strain (50%) at 10th cycle. Although the sample after copolymerization with PEGMEMA (sample **4**) is more stretchable than sample **2** (211% *vs* 88%), the low tensile strength may limit the use in practical application as a free-standing film. The functional polymer membrane with MPA-Li^+ as the monomer (sample **7**) exhibited enhanced mechanical performance, i.e., higher extensibility (142% *vs* 88%) and ultimate tensile strength (0.64 MPa *vs* 0.37 MPa), which should be attributed to its high molecular flexibility.[66] The MPA-Li^+ based SICPE (sample **7**) has higher Young's modulus (0.53 *vs* 0.32 MPa) and ultimate tensile strength (0.65 vs 0.32

MPa) than MPA-Na^+ based SICPE (sample **9**), probably due to the presence of coordinative ionic interaction of Li^+ with PEO.[65, 69]

Table 2. Combined Young's modulus, elongation, toughness, and ultimate tensile strength of the stretchable single-ion conducting polymer electrolyte membranes.

NO.	Sample	Et(MPa)	Eb(%)	Toughness (MJ/m3)	Tensile strength (MPa)
2	PDMS-poly(STF-Li^+-*r*-PEGMA)$_{20}$-PDMS$_{10}$	0.66±0.05	88.1±5.5	0.18±0.02	0.37±0.03
3	PDMS-poly(STF-Li^+-*r*-PEGMA)$_{50}$-PDMS$_{10}$	0.68±0.06	81.4±3.2	0.15±0.01	0.34±0.01
4	PDMS-poly(STF-Li^+-*r*-PEGMEMA)$_{20}$-PDMS$_{10}$	0.15±0.01	211.5±12.4	0.12±0.01	0.09±0.01
5	PDMS-poly(STF-Li^+-*r*-PEG)$_{20}$-PDMS$_{10}$	0.21±0.01	151.9±8.6	0.14±0.01	0.16±0.01
6	PDMS-poly(MPA-Li^+-*r*-PEGMA)$_{20}$-PDMS$_5$	0.47±0.01	141.7±4.1	0.41±0.03	0.62±0.06
7	PDMS-poly(MPA-Li^+-*r*-PEGMA)$_{20}$-PDMS$_{10}$	0.53±0.06	169.4±4.4	0.47±0.06	0.65±0.05
8	PDMS-poly(MPA-Li^+-*r*-PEGMA)$_{20}$-PDMS$_{20}$	1.60±0.08	115.1±8.5	0.50±0.03	0.73±0.02
9	PDMS-poly(MPA-Na^+-*r*-PEGMA)$_{20}$-PDMS$_{10}$	0.32±0.02	252.4±10.4	0.40±0.01	0.36±0.01

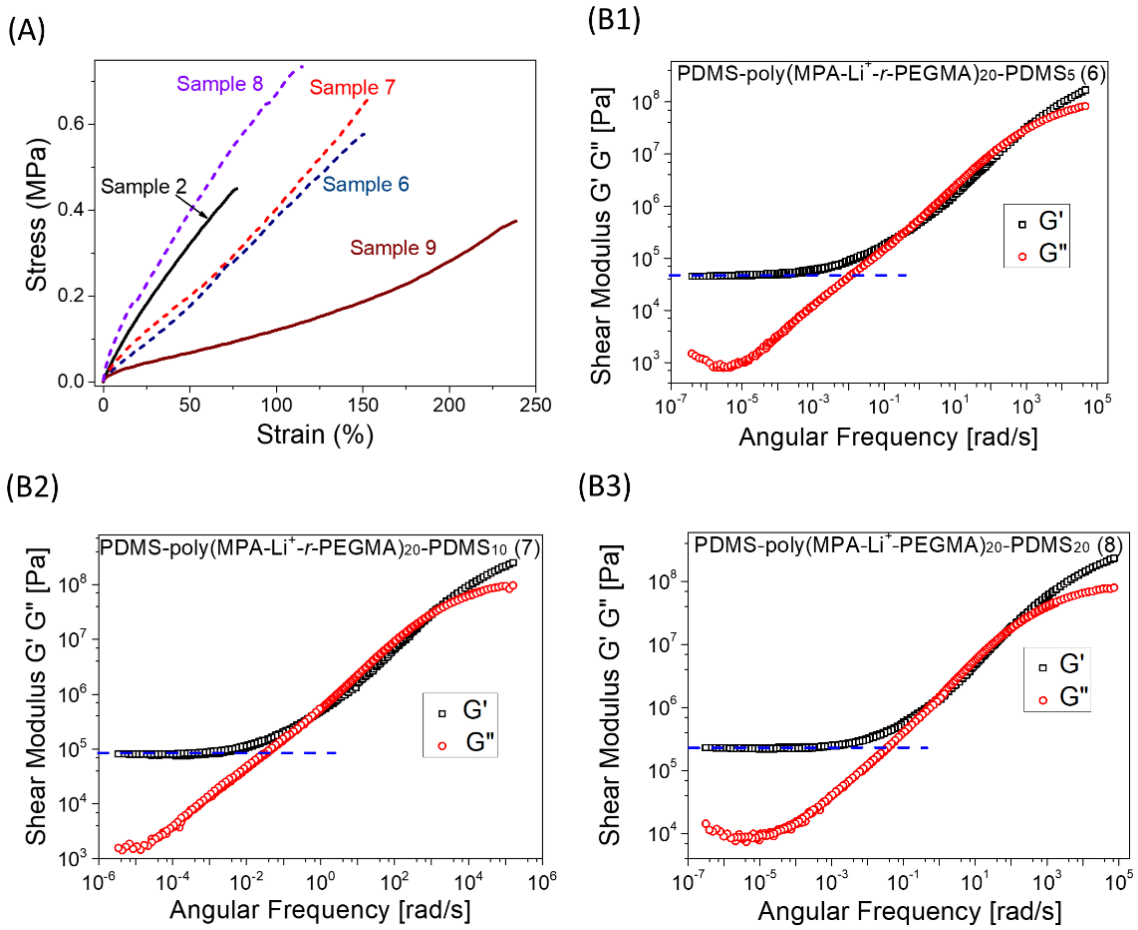

Figure 2. (A) Tensile test of elastic polymer membranes, see (Table 2) for combined results; (B) Rheology analysis of elastic polymer membranes (6, 7 and 8, master curves with reference temperature at 283.15K).

Adjusting the crosslinking density has been demonstrated as a useful strategy to tune the mechanical performance of elastic polymer membranes, and our previous studies showed that crosslinking density was adjustable by modifying the MW of telechelic PDMS.[12-13] Herein, the crosslinking density is also tuned by changing the molar ratio of elastic crosslinker (**V**) to grafted functional copolymers (**IV**). Using the grafted block copolymer, PDSM-poly(MPA-Li^+-*r*-PEGMA)$_{20}$, functional polymer membranes with molar ratio of V to IV being 5:1, 10:1 and 20:1 were fabricated (Table 2, sample **6, 7, 8**). As manifested by the storage-modulus plateau in the rheology data of obtained polymer films (Figure 2(B)), the increased amount of crosslinker leads to higher crosslinking density, from 1.38×10^{-5}, 2.31×10^{-5} to 6.46×10^{-5} mol/cm^3. As expected, the Young's modulus, toughness, and tensile strength significantly increased with the crosslinking density. However, the extensibility did not show an obvious correlation with the crosslinking density, which was similar to our previously reported isocyanate crosslinked PDMS membranes that no direct correlation was observed between the M_n of PDMS and elongation before breaks.[13] This can be explained by the increase in the crosslinking density that restricts the polymer segmental dynamics and makes the membrane less extensible. In the meantime, increasing the weight ratio of low-T_g component by the addition of PDMS crosslinker leads to lower T_g value of the system that tend to shorten the segmental relaxation time. Therefore, T_g value and extensibility of the membranes can be tailored by the balance of crosslinking density and weight ratio of low T_g polymer composition.

Conductivity measurement and battery testing. Ionic conductivity (σ) of the obtained SICPEs was measured using a broadband dielectric spectroscopy (BDS). To ensure an accurate ionic conductivity measurement with completely dried samples, all the samples were dried in a vacuum oven at 80 °C for at least three days. More than 30 scans at high temperature (~120 °C) were performed to ensure the reproducible data before starting the measurement with cooling and heating cycles. Moreover, the ionic conductivities at the same temperature during cooling cycle and heating cycle were confirmed to be the

same before the data can be utilized. The real part of conductivity (σ') (Figure 3(A)) exhibits three visible regions: electrode polarization at low frequency, dc-conductivity (σ_{dc}) in the frequency-independent region, and power law behavior (ac-conductivity) at high frequency.[77] The temperature dependence of dc-conductivity (σ_{dc}) exhibits a crossover from an Arrhenius behavior to Vogel-Fulcher-Tammann (VFT) behavior upon heating above T_g (Figure 3(B)). This behavior is typical for polymeric electrolytes, which provides an alternative method for the measurement of T_g (see the fitting curve for sample **2** in Figure 3(B)). The measured T_g value of the sample **2** from BDS is consistent with that from DSC (249 K/-25°C *vs* -17.5 °C), and significant difference in the heating rate (~ 0.33 °C/min for BDS *vs* 5 °C/min for DSC) might be the main reason for their slight difference. As illustrated in the Table S1, the T_g values obtained from the two different methods are comparable for all of the measured SICPEs.

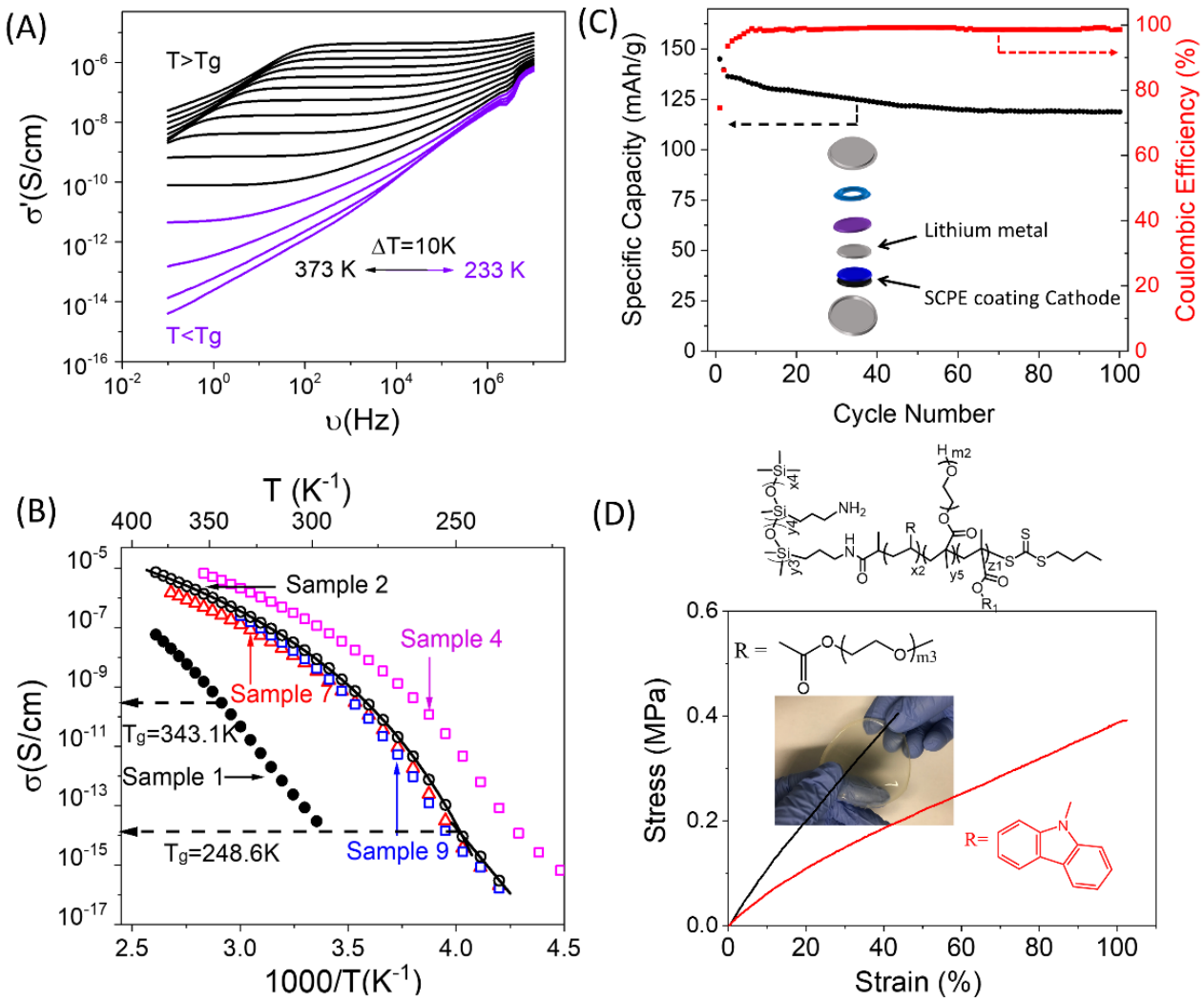

Figure 3. (A) Dielectric relaxation spectra of sample **2** in the measured above (black lines) and below (purple lines) T_g=248.6 K presented at the conductivity *vs* frequency; (B) Temperature dependence of conductivity (σ_{dc}) of the sample **1**, **2**, **4**, **7** and **9** (See table 1 for detailed sample names); (C) Specific capacity and coulombic efficiency of the cell with sample **2** as the solid electrolyte with 0.1C at the temperature of 65 °C; (D) Chemical structure (see whole structure in Scheme 1(B)) and its corresponding tensile test of the stretchable polymers with PEO or poly(vinyl carbazole) as the functionalities.

To investigate the relationship between the structural relaxation and diffusion of Li^+ in the polymeric anions, a comparison between the segmental relaxation time (τ_0) and conductivity relaxation time (τ_σ) has been plotted against the temperature dependence (Figure S10). The conductivity relaxation time (τ_σ) is determined by the peak maximum of the loss electric modulus (M″ from BDS) using the equation $\tau_\sigma = 1/2\pi f_{max}$, whereas the segmental relaxation time (τ_0) is calculated from the frequency corresponding to the cross point of storage modulus (G′) and loss modulus (G″) in the rheology test (See

Figure S11 for one example). More than two-order difference between the τ_σ and τ_0 for PDMS-poly(STF-Li^+-*r*-PEGMA)$_{20}$-PDMS$_{10}$ (sample **2**) indicates that the ionic dynamics are faster than segmental dynamics, which is a typical decoupling behavior. Unfortunately, the brittle nature of the PDMS-poly(STF-Li^+)$_{20}$-PDMS$_{10}$ (sample **1)** makes the rheology test impossible for determining its τ_0 value. An alternative method is comparing their dc-conductivity (σ_{dc}) at T_g, and the values higher than 10^{-15} S/cm at T_g usually indicates decoupled ion conduction. From this method, around five orders of decoupling between segmental and ionic dynamics is evident for the sample **1**. This is consistent with previous reports that polymer electrolytes with more rigid structure (higher T_g) exhibit more significant decoupling.[61, 78]

Although less significant decoupling was observed after copolymerization with PEGMA, the dc-conductivity of PDMS-poly(STF-Li^+-*r*-PEGMA)$_{20}$-PDMS$_{10}$ (sample **2)** at the same temperature is significantly higher than that of sample **1** due to its significantly lower T_g values. Aside from the T_g effect, the density functional theory (DFT) computed interaction of Li^+ and PEGMA (-3.0 eV) also facilitates the dissociation of the Li^+ from its counter ions. Computational calculations also demonstrated that although stable three-body interactions are present (Li^+-STF-PEGMA, -7.7 eV), the higher chance of two-body system (including Li^+-STF, Li^+-PEGMA, and STF-PEGMA, -10.2 eV in total) suggest the dynamic interaction of the obtained SICPEs. Increasing DP_n of the side chain from 20 to 50 leads to increased weight ratio of functional units (from 79.2% to 90.8% in weight) and improved σ_{dc} of obtained product (sample **3** *vs* sample **2,** Figure S12). The comparative ionic conductivities of SICPEs with different crosslinking densities (sample **6**, **7** and **8**) is consistent with their comparative T_g values (Figure S13). Different monomers (MPA-Li^+ *vs* STF-Li^+) showed negligible difference in conductivity after copolymerizing with the same ratio of PEGMA (sample **7** *vs* sample **2** in Figure 3(B)). This is consistent with DFT computed interaction energies between MPA and Li^+, and STF and Li^+, which are essentially comparable (-6.3 eV and -6.4 eV, respectively). The PDMS-poly(STF-Li^+-*r*-PEGMEMA)$_{20}$-PDMS$_{10}$ (sample **4**) exhibited around 5 times conductivity improvement due to lower T_g value and higher conformation freedom than that of sample **2**, while sample **4** does not form a free-standing film. With

equivalent molar ratio of PEGMA and PEGMEMA, PDMS-poly(STF-Li^+-*r*-PEG)$_{20}$-PDMS$_{10}$ (sample **5**) is a stretchable free-standing polymer film, and its dc-conductivity is comparable with that of sample **2** (See Figure S14).

The lithium-ion transference number (strictly speaking, transport number using this method) of PDMS-poly(STF-Li^+-*r*-PEGMA)$_{20}$-PDMS$_{10}$ (sample **2)** was measured to be 0.79 using the Bruce-Vincent method (see Table S2). The electrochemical stability of elastic SICPEs was evaluated using the cell sandwiched between the metallic lithium and stainless steel (Figure S15). With initial oxidation occurs at 3.5V, the successive cycles do not exhibit any side reactions until 4.2V, which may indicate the formation of passivation layer after initial cycle that prevent further oxidation of the SICPEs membrane. Herein, we chose $LiFePO_4$ as the cathode and in-situ formation of sample **2** was also performed on the cathode, which is important to decrease the interfacial resistance.[64] Moreover, instead of using conventional PVDF binder, SICPE (PDMS-poly(STF-Li^+-*r*-PEGMA)$_{20}$) was employed to ensure the efficient Li^+ transfer in the cathode (60wt% $LiFePO_4$, 30wt% PDMS-poly(STF-Li^+-*r*-PEGMA)$_{20}$, and 10wt% carbon black).[63] With lithium as the counter electrode, the interfacial resistances of solid electrolyte with $LiFeO_4$ cathode and Li metal anode were calculated to be 5040 Ω and 2130 Ω, respectively using the constant phase element (see details in Supporting Information). The galvanostatic test of the assembled cell is performed between 3.8 V to 2.5 V with specific capacity and voltage profile shown in Figure 3(C) and Figure S17. Significant capacity loss and lower coulombic efficiency observed for the first two cycles can be explained by the formation of a passivation layer at electrode interface that consumes some lithium ion.[63] More stable cycling performance was obtained in the following cycles, and the capacity retention is calculated to be 81.5% after 100 cycles (Figure 3(C)).

Stretchable polymers with other functionalities. The designed strategy on molecular-level stretchable functional polymer is not only useful for the fabrication of stretchable SICPEs (that can be used in stretchable batteries/electronics), but also is applicable for other kinds of stretchable functional polymeric

materials. To demonstrate the versatility of the approach, we also fabricated the stretchable materials with other kinds of functionalities. As the first example, carbazole functionalized polymers were grafted onto PDMS backbone. Poly(vinyl carbazole) possesses semiconducting property and other unique photochemical, electro-optical, and electrochemical properties.[79-82] From PDMS-backboned macro RAFT-CTA (compound **III)**, RAFT polymerization of vinyl carbazole and PEGMA (molar ratio=3:1) will render the grafted block copolymer PDMS-poly(Cbz-*r*-PEGMA)$_{20}$ with ^{1}H NMR spectrum shown in Figure S12. Further crosslinking by elastic PDMS will render an elastic polymer membrane with around 100% elongation before breaks (Figure 3(D)).

PEO based polymer membranes are also useful for many fields, including solid electrolyte, anti-fouling surface and gas-separation membranes.[83-85] Our previous work demonstrated that incorporation of PEO will significantly improve the gas selectivity for the CO_2/N_2 separation due to its CO_2-philic nature.[85] With PEGMA and PEGMEMA (molar ratio=1:1) as the side chains, the elastic polymer membranes have been fabricated by using the same procedure described above. As expected, good extensibility (~50%) and modulus (Young's modulus=1.00±0.09MPa) was obtained for PDMS-poly(PEG)$_{20}$-PDMS$_{10}$ as shown in Figure 3(D). The gas separation performance of the obtained elastic membrane was evaluated for one of the potential applications (see Figure S13). From the representative plot of pressure increase, gas selectivity of the elastic polymer membranes with around 75% PEO in weight exhibited CO_2/N_2=36.5, which is a relatively high value among the elastic gas-separation membranes.[13, 85]

CONCLUSION

A robust platform on the fabrication of a molecular-level stretchable functional polymeric material has been developed *via* designing a crosslinked grafted block copolymer. The rational design allowed to successfully prepare a series of stretchable single-ion (Li^+ and Na^+) conducting polymeric materials with a random copolymer of PEGMA and Sty-Li^+ (or MPA-Li^+ or MPA-Na^+) as the side chains and elastic PDMS as the polymer backbone and crosslinker. All of the membranes exhibited good extensibility before

breaks. The mechanical properties of the elastic membranes are well-tunable by changing the molar ratio of elastic PDMS cross-linker and grafted block copolymers: higher molar ratio will render higher crosslinking density and hence higher Young's modulus and tensile strength. Both copolymerization with PEO and increasing the side chain length improve the dc-conductivity at the same temperature, while changing the monomer types (STF-Li^+ *vs* MPA-Li^+) does not significantly affect its performance. Galvanostatic test of the assembled cell utilizing the fabricated SICPEs revealed satisfactory cycling performance with capacity retention at 81.5% after 100 cycles. The developed approach has also been proved being an important platform for synthesizing stretchable materials with other functionalities, such as poly(vinyl carbazole) based semiconductor and PEO based gas-separation membranes.

With significant advantages of SICPEs in battery applications, the stretchable SICPEs provide the possibility to improve the overall performance of future stretchable batteries/devices. The versatile molecular-level design of the stretchable functional materials will also be insightful for both fundamental understanding and various other applications including but not limited to stretchable devices, coating and membranes.

Nomenclature

PDMS-NH_2 (**I**): commercially available PDMS with numerous amine side groups; PDMS-RAFT (**III**)**:** partially RAFT-CTA functionalized PDMS-NH_2, herein, DG_n of RAFT-CTA on the PDMS-NH_2 is fixed as 29; PDMS-poly(STF-Li^+-*r*-PEGMA)$_m$ (**IV**): random copolymer of STF-Li^+ and PEGMA grafted PDMS, the DP_n of the random copolymer is m; PDMS-poly(STF-Li^+-*r*-PEGMA)$_m$-PDMS$_n$: elastic polymer membrane of PDMS crosslinked PDMS-poly(STF-Li^+-*r*-PEGMA)$_m$ and molar ratio of PDMS crosslinker to PDMS-poly(STF-Li^+-*r*-PEGMA)$_m$ is n.

ASSOCIATED CONTENT

Supporting Information. ^{1}H NMR spectra, TGA, DSC, SAXS, rheology, BDS, gas-separation data, experimental section and simulation details are provided in Supporting Information. This material is available free of charge via the Internet at http://pubs.acs.org."

AUTHOR INFORMATION

Corresponding Author

* Dr. Cao (caop@ornl.gov) and Dr. Saito (saitot@ornl.gov)

ACKNOWLEDGMENT

This study was supported by the U.S. Department of Energy, Office of Science, Basic Energy Sciences, Materials Sciences and Engineering Division. GY and JN acknowledges financial support for the electrochemical characterization of the membranes by the U.S. Department of Energy, Office of Electricity and Reliability. KX acknowledges financial support for the rheology measurement from NSF Polymer program (DMR-1408811). JT and KDV would like to acknowledge the University of Tennessee for financial support (start-up grant) and the Advanced Computer Facility (ACF) of the University of Tennessee for DFT calculation. A portion of this research was conducted at the Center for Nanophase Materials Sciences, which is a DOE Office of Science User Facility.

REFERENCES

1. Liu, W.; Chen, J.; Chen, Z.; Liu, K.; Zhou, G.; Sun, Y.; Song, M. S.; Bao, Z.; Cui, Y., Stretchable Lithium‐Ion Batteries Enabled by Device‐Scaled Wavy Structure and Elastic‐Sticky Separator. *Adv. Energy Mater.* **2017,** *7* (21), 1701076.
2. Kaltenbrunner, M.; White, M. S.; Głowacki, E. D.; Sekitani, T.; Someya, T.; Sariciftci, N. S.; Bauer, S., Ultrathin and lightweight organic solar cells with high flexibility. *Nat. Commun.* **2012,** *3*, 770.
3. Liu, W.; Song, M. S.; Kong, B.; Cui, Y., Flexible and Stretchable Energy Storage: Recent Advances and Future Perspectives. *Adv. Mater.* **2016,** *29* (1), 1603436.
4. Wang, L.; Zhang, Y.; Pan, J.; Peng, H., Stretchable lithium-air batteries for wearable electronics. *J.Mater. Chem. A* **2016,** *4* (35), 13419-13424.
5. Nishide, H.; Oyaizu, K., Toward Flexible Batteries. *Science* **2008,** *319* (5864), 737.
6. Xu, S.; Zhang, Y.; Cho, J.; Lee, J.; Huang, X.; Jia, L.; Fan, J. A.; Su, Y.; Su, J.; Zhang, H.; Cheng, H.; Lu, B.; Yu, C.; Chuang, C.; Kim, T.-i.; Song, T.; Shigeta, K.; Kang, S.; Dagdeviren, C.; Petrov, I.; Braun, P. V.; Huang, Y.; Paik, U.; Rogers, J. A., Stretchable batteries with self-similar serpentine interconnects and integrated wireless recharging systems. *Nat. Commun.* **2013,** *4*, 1543.
7. Ma, R.; Feng, J.; Yin, D.; Sun, H.-B., Highly efficient and mechanically robust stretchable polymer solar cells with random buckling. *Org. Electron.* **2017,** *43*, 77-81.
8. Zamarayeva, A. M.; Ostfeld, A. E.; Wang, M.; Duey, J. K.; Deckman, I.; Lechêne, B. P.; Davies, G.; Steingart, D. A.; Arias, A. C., Flexible and stretchable power sources for wearable electronics. *Sci. Adv.* **2017,** *3* (6).
9. Trung Tran, Q.; Lee, N. E., Flexible and Stretchable Physical Sensor Integrated Platforms for Wearable Human‐Activity Monitoringand Personal Healthcare. *Adv. Mater.* **2016,** *28* (22), 4338-4372.
10. Kim, M.; Lee, C.; Jang, J., Fabrication of Highly Flexible, Scalable, and High‐Performance Supercapacitors Using Polyaniline/Reduced Graphene Oxide Film with Enhanced Electrical Conductivity and Crystallinity. *Adv. Funct. Mater.* **2013,** *24* (17), 2489-2499.
11. Zhao, J.; Han, S.; Yang, Y.; Fu, R.; Ming, Y.; Lu, C.; Liu, H.; Gu, H.; Chen, W., Passive and Space-Discriminative Ionic Sensors Based on Durable Nanocomposite Electrodes toward Sign Language Recognition. *ACS Nano* **2017,** *11* (9), 8590-8599.
12. Cao, P. F.; Li, B.; Hong, T.; Townsend, J.; Qiang, Z.; Xing, K.; Vogiatzis Konstantinos, D.; Wang, Y.; Mays Jimmy, W.; Sokolov Alexei, P.; Saito, T., Superstretchable, Self‐Healing Polymeric Elastomers with Tunable Properties. *Adv. Funct. Mater.* **2018,** *28* (22), 1800741.
13. Cao, P.-F.; Li, B.; Hong, T.; Xing, K.; Voylov, D. N.; Cheng, S.; Yin, P.; Kisliuk, A.; Mahurin, S. M.; Sokolov, A. P.; Saito, T., Robust and Elastic Polymer Membranes with Tunable Properties for Gas Separation. *ACS. Appl. Mater. Interfaces* **2017,** *9* (31), 26483-26491.
14. Sekitani, T.; Nakajima, H.; Maeda, H.; Fukushima, T.; Aida, T.; Hata, K.; Someya, T., Stretchable active-matrix organic light-emitting diode display using printable elastic conductors. *Nat. Mater.* **2009,** *8*, 494.
15. Kim, J.; Shim Hyung, J.; Yang, J.; Choi Moon, K.; Kim Dong, C.; Kim, J.; Hyeon, T.; Kim, D. H., Ultrathin Quantum Dot Display Integrated with Wearable Electronics. *Adv. Mater.* **2017,** *29* (38), 1700217.
16. Trung Tran, Q.; Lee, N. E., Recent Progress on Stretchable Electronic Devices with Intrinsically Stretchable Components. *Adv. Mater.* **2016,** *29* (3), 1603167.
17. Benight, S. J.; Wang, C.; Tok, J. B. H.; Bao, Z., Stretchable and self-healing polymers and devices for electronic skin. *Prog. Polym. Sci.* **2013,** *38* (12), 1961-1977.
18. Park, M.; Im, J.; Shin, M.; Min, Y.; Park, J.; Cho, H.; Park, S.; Shim, M.-B.; Jeon, S.; Chung, D.-Y.; Bae, J.; Park, J.; Jeong, U.; Kim, K., Highly stretchable electric circuits from a composite material of silver nanoparticles and elastomeric fibres. *Nat. Nanotechnol.* **2012,** *7*, 803.
19. Ge, J.; Yao, H. B.; Wang, X.; Ye, Y. D.; Wang, J. L.; Wu, Z. Y.; Liu, J. W.; Fan, F. J.; Gao, H. L.; Zhang, C. L.; Yu, S. H., Stretchable Conductors Based on Silver Nanowires: Improved Performance through a Binary Network Design. *Angew. Chem. Int. Ed.* **2013,** *52* (6), 1654-1659.
20. Sadasivuni, K. K.; Ponnamma, D.; Thomas, S.; Grohens, Y., Evolution from graphite to graphene elastomer composites. *Prog. Polym. Sci.* **2014,** *39* (4), 749-780.
21. Kujawski, M.; Pearse, J. D.; Smela, E., Elastomers filled with exfoliated graphite as compliant electrodes. *Carbon* **2010,** *48* (9), 2409-2417.
22. Hansen, T. S.; West, K.; Hassager, O.; Larsen, N. B., Highly Stretchable and Conductive Polymer Material Made from Poly(3,4‐ethylenedioxythiophene) and Polyurethane Elastomers. *Adv. Funct. Mater.* **2007,** *17* (16), 3069-3073.
23. Wang, C.; Zheng, W.; Yue, Z.; Too Chee, O.; Wallace Gordon, G., Buckled, Stretchable Polypyrrole Electrodes for Battery Applications. *Adv. Mater.* **2011,** *23* (31), 3580-3584.
24. Chen, Q.; Cao, P. F.; Advincula Rigoberto, C., Mechanically Robust, Ultraelastic Hierarchical Foam with Tunable Properties via 3D Printing. *Adv. Funct. Mater.* **2018,** *28* (21), 1800631.
25. Yamada, T.; Hayamizu, Y.; Yamamoto, Y.; Yomogida, Y.; Izadi-Najafabadi, A.; Futaba, D. N.; Hata, K., A stretchable carbon nanotube strain sensor for human-motion detection. *Nat. Nanotechnol.* **2011,** *6*, 296.
26. Chun, K.-Y.; Oh, Y.; Rho, J.; Ahn, J.-H.; Kim, Y.-J.; Choi, H. R.; Baik, S., Highly conductive, printable and stretchable composite films of carbon nanotubes and silver. *Nat. Nanotechnol.* **2010,** *5*, 853.
27. Yu, C.; Wang, Z.; Yu, H.; Jiang, H., A stretchable temperature sensor based on elastically buckled thin film devices on elastomeric substrates. *Appl. Phys. Lett.* **2009,** *95* (14), 141912.

28. Pang, C.; Lee, G.-Y.; Kim, T.-i.; Kim, S. M.; Kim, H. N.; Ahn, S.-H.; Suh, K.-Y., A flexible and highly sensitive strain-gauge sensor using reversible interlocking of nanofibres. *Nat. Mater.* **2012,** *11*, 795.
29. Wu, H.; Su, Z.; Shi, M.; Miao, L.; Song, Y.; Chen, H.; Han, M.; Zhang, H., Self‐Powered Noncontact Electronic Skin for Motion Sensing. *Adv. Funct. Mater.* **2017,** *28* (6), 1704641.
30. Wang, X.; Gu, Y.; Xiong, Z.; Cui, Z.; Zhang, T., Silk‐Molded Flexible, Ultrasensitive, and Highly Stable Electronic Skin for Monitoring Human Physiological Signals. *Adv. Mater.* **2013,** *26* (9), 1336-1342.
31. Li, C.; Pan, L.; Deng, C.; Cong, T.; Yin, P.; Wu, Z., A highly sensitive and wide-range pressure sensor based on a carbon nanocoil network fabricated by an electrophoretic method. *J. Mater. Chem. C* **2017,** *5* (45), 11892-11900.
32. Chou, H.-H.; Nguyen, A.; Chortos, A.; To, J. W. F.; Lu, C.; Mei, J.; Kurosawa, T.; Bae, W.-G.; Tok, J. B. H.; Bao, Z., A chameleon-inspired stretchable electronic skin with interactive colour changing controlled by tactile sensing. *Nat. Commun.* **2015,** *6*, 8011.
33. Jeong, G. S.; Baek, D.-H.; Jung, H. C.; Song, J. H.; Moon, J. H.; Hong, S. W.; Kim, I. Y.; Lee, S.-H., Solderable and electroplatable flexible electronic circuit on a porous stretchable elastomer. *Nat. Commun.* **2012,** *3*, 977.
34. Lou, Z.; Chen, S.; Wang, L.; Shi, R.; Li, L.; Jiang, K.; Chen, D.; Shen, G., Ultrasensitive and ultraflexible e-skins with dual functionalities for wearable electronics. *Nano Energy* **2017,** *38*, 28-35.
35. Park, K.; Lee, D. K.; Kim, B. S.; Jeon, H.; Lee, N. E.; Whang, D.; Lee, H. J.; Kim Youn, J.; Ahn, J. H., Stretchable, Transparent Zinc Oxide Thin Film Transistors. *Adv. Funct. Mater.* **2010,** *20* (20), 3577-3582.
36. Kunugi, Y.; Yamada, Y.; Horiuchi, H.; Hiratsuka, H.; Ohshita, J., OFET Characteristics of Stretched Poly(3-hexylthiophene) Films. *Electrochemistry* **2010,** *78* (3), 191-193.
37. Shin, M.; Oh Jin, Y.; Byun, K. E.; Lee, Y. J.; Kim, B.; Baik, H. K.; Park, J. J.; Jeong, U., Polythiophene Nanofibril Bundles Surface‐Embedded in Elastomer: A Route to a Highly Stretchable Active Channel Layer. *Adv. Mater.* **2015,** *27* (7), 1255-1261.
38. Wenger, B.; Tétreault, N.; Welland, M. E.; Friend, R. H., Mechanically tunable conjugated polymer distributed feedback lasers. *Appl. Phys. Lett.* **2010,** *97* (19), 193303.
39. Song, E.; Kang, B.; Choi Hyun, H.; Sin Dong, H.; Lee, H.; Lee Wi, H.; Cho, K., Stretchable and Transparent Organic Semiconducting Thin Film with Conjugated Polymer Nanowires Embedded in an Elastomeric Matrix. *Adv. Electron. Mater.* **2015,** *2* (1), 1500250.
40. Wang, T.; Wang, R.; Cheng, Y.; Sun, J., Quasi In Situ Polymerization To Fabricate Copper Nanowire-Based Stretchable Conductor and Its Applications. *ACS. Appl. Mater. Interfaces* **2016,** *8* (14), 9297-9304.
41. Lee, Y.; Shin, M.; Thiyagarajan, K.; Jeong, U., Approaches to Stretchable Polymer Active Channels for Deformable Transistors. *Macromolecules* **2016,** *49* (2), 433-444.
42. Chortos, A.; Zhu, C.; Oh, J. Y.; Yan, X.; Pochorovski, I.; To, J. W. F.; Liu, N.; Kraft, U.; Murmann, B.; Bao, Z., Investigating Limiting Factors in Stretchable All-Carbon Transistors for Reliable Stretchable Electronics. *ACS Nano* **2017,** *11* (8), 7925-7937.
43. Xu, J.; Wang, S.; Wang, G.-J. N.; Zhu, C.; Luo, S.; Jin, L.; Gu, X.; Chen, S.; Feig, V. R.; To, J. W. F.; Rondeau-Gagné, S.; Park, J.; Schroeder, B. C.; Lu, C.; Oh, J. Y.; Wang, Y.; Kim, Y.-H.; Yan, H.; Sinclair, R.; Zhou, D.; Xue, G.; Murmann, B.; Linder, C.; Cai, W.; Tok, J. B. H.; Chung, J. W.; Bao, Z., Highly stretchable polymer semiconductor films through the nanoconfinement effect. *Science* **2017,** *355* (6320), 59.
44. Wang Ging‐Ji, N.; Gasperini, A.; Bao, Z., Stretchable Polymer Semiconductors for Plastic Electronics. *Adv. Electron. Mater.* **2018,** *4* (2), 1700429.
45. Wang Ging‐Ji, N.; Shaw, L.; Xu, J.; Kurosawa, T.; Schroeder Bob, C.; Oh Jin, Y.; Benight Stephanie, J.; Bao, Z., Inducing Elasticity through Oligo‐Siloxane Crosslinks for Intrinsically Stretchable Semiconducting Polymers. *Adv. Funct. Mater.* **2016,** *26* (40), 7254-7262.
46. Müller, C.; Goffri, S.; Breiby, D. W.; Andreasen, J. W.; Chanzy, H. D.; Janssen, R. A. J.; Nielsen, M. M.; Radano, C. P.; Sirringhaus, H.; Smith, P.; Stingelin‐Stutzmann, N., Tough, Semiconducting Polyethylene‐poly(3‐hexylthiophene) Diblock Copolymers. *Adv. Funct. Mater.* **2007,** *17* (15), 2674-2679.
47. Peng, R.; Pang, B.; Hu, D.; Chen, M.; Zhang, G.; Wang, X.; Lu, H.; Cho, K.; Qiu, L., An ABA triblock copolymer strategy for intrinsically stretchable semiconductors. *J. Mater. Chem. C* **2015,** *3* (15), 3599-3606.
48. Richey, F. W.; Dyatkin, B.; Gogotsi, Y.; Elabd, Y. A., Ion Dynamics in Porous Carbon Electrodes in Supercapacitors Using in Situ Infrared Spectroelectrochemistry. *J. Am. Chem. Soc.* **2013,** *135* (34), 12818-12826.
49. Shin, D. W.; Guiver, M. D.; Lee, Y. M., Hydrocarbon-Based Polymer Electrolyte Membranes: Importance of Morphology on Ion Transport and Membrane Stability. *Chem. Rev.* **2017,** *117* (6), 4759-4805.
50. Bocharova, V.; Wojnarowska, Z.; Cao, P.-F.; Fu, Y.; Kumar, R.; Li, B.; Novikov, V. N.; Zhao, S.; Kisliuk, A.; Saito, T.; Mays, J. W.; Sumpter, B. G.; Sokolov, A. P., Influence of Chain Rigidity and Dielectric Constant on the Glass Transition Temperature in Polymerized Ionic Liquids. *J. Phys. Chem. B* **2017,** *121* (51), 11511-11519.
51. Lu, Y.; Tikekar, M.; Mohanty, R.; Hendrickson, K.; Ma, L.; Archer Lynden, A., Stable Cycling of Lithium Metal Batteries Using High Transference Number Electrolytes. *Adv. Energy Mater.* **2015,** *5* (9), 1402073.
52. Sun, X.-G.; Kerr, J. B., Synthesis and Characterization of Network Single Ion Conductors Based on Comb-Branched Polyepoxide Ethers and Lithium Bis(allylmalonato)borate. *Macromolecules* **2006,** *39* (1), 362-372.
53. Buss, H. G.; Chan, S. Y.; Lynd, N. A.; McCloskey, B. D., Nonaqueous Polyelectrolyte Solutions as Liquid Electrolytes with High Lithium Ion Transference Number and Conductivity. *ACS Energy Lett.* **2017,** *2* (2), 481-487.
54. Li, S.; Mohamed, A. I.; Pande, V.; Wang, H.; Cuthbert, J.; Pan, X.; He, H.; Wang, Z.; Viswanathan, V.; Whitacre, J. F.; Matyjaszewski, K., Single-Ion Homopolymer Electrolytes with High Transference Number Prepared by Click Chemistry and Photoinduced Metal-Free Atom-Transfer Radical Polymerization. *ACS Energy Lett.* **2018,** *3* (1), 20-27.
55. Zhang, H.; Li, C.; Piszcz, M.; Coya, E.; Rojo, T.; Rodriguez-Martinez, L. M.; Armand, M.; Zhou, Z., Single lithium-ion conducting solid polymer electrolytes: advances and perspectives. *Chem. Soc. Rev.* **2017,** *46* (3), 797-815.
56. Thomas, K. E.; Sloop, S. E.; Kerr, J. B.; Newman, J., Comparison of lithium-polymer cell performance with unity and nonunity transference numbers. *J. Power Sources* **2000,** *89* (2), 132-138.
57. Zhao, C.-Z.; Zhang, X.-Q.; Cheng, X.-B.; Zhang, R.; Xu, R.; Chen, P.-Y.; Peng, H.-J.; Huang, J.-Q.; Zhang, Q., An anion-immobilized composite electrolyte for dendrite-free lithium metal anodes. *Proc. Natl. Acad. Sci.* **2017,** *114* (42), 11069.
58. Diederichsen, K. M.; McShane, E. J.; McCloskey, B. D., Promising Routes to a High Li+ Transference Number Electrolyte for Lithium Ion Batteries. *ACS Energy Lett.* **2017,** *2* (11), 2563-2575.
59. Chereddy, S.; Chinnam, P. R.; Chatare, V.; diLuzio, S. P.; Gobet, M. P.; Greenbaum, S. G.; Wunder, S. L., An alternative route to single ion conductivity using multi-ionic salts. *Mater. Horizons* **2018,** *5* (3), 461-473.
60. Ma, Q.; Zhang, H.; Zhou, C.; Zheng, L.; Cheng, P.; Nie, J.; Feng, W.; Hu, Y. S.; Li, H.; Huang, X.; Chen, L.; Armand, M.; Zhou, Z., Single Lithium‐Ion Conducting Polymer Electrolytes Based on a Super‐Delocalized Polyanion. *Angew. Chem. Int. Ed.* **2016,** *55* (7), 2521-2525.
61. Cao, P.-F.; Wojnarowska, Z.; Hong, T.; Carroll, B.; Li, B.; Feng, H.; Parsons, L.; Wang, W.; Lokitz, B. S.; Cheng, S.; Bocharova, V.; Sokolov, A. P.; Saito, T., A star-shaped single lithium-ion conducting copolymer by grafting a POSS nanoparticle. *Polymer* **2017,** *124*, 117-127.
62. Kim, Y.; Kwon, S. J.; Jang, H.-k.; Jung, B. M.; Lee, S. B.; Choi, U. H., High Ion Conducting Nanohybrid Solid Polymer Electrolytes via Single-Ion Conducting Mesoporous Organosilica in Poly(ethylene oxide). *Chem. Mater.* **2017,** *29* (10), 4401-4410.

63. Porcarelli, L.; Shaplov, A. S.; Salsamendi, M.; Nair, J. R.; Vygodskii, Y. S.; Mecerreyes, D.; Gerbaldi, C., Single-Ion Block Copoly(ionic liquid)s as Electrolytes for All-Solid State Lithium Batteries. *ACS. Appl. Mater. Interfaces* **2016,** *8* (16), 10350-10359.
64. Porcarelli, L.; Shaplov, A. S.; Bella, F.; Nair, J. R.; Mecerreyes, D.; Gerbaldi, C., Single-Ion Conducting Polymer Electrolytes for Lithium Metal Polymer Batteries that Operate at Ambient Temperature. *ACS Energy Lett.* **2016,** *1* (4), 678-682.
65. Rojas, A. A.; Inceoglu, S.; Mackay, N. G.; Thelen, J. L.; Devaux, D.; Stone, G. M.; Balsara, N. P., Effect of Lithium-Ion Concentration on Morphology and Ion Transport in Single-Ion-Conducting Block Copolymer Electrolytes. *Macromolecules* **2015,** *48* (18), 6589-6595.
66. Devaux, D.; Liénafa, L.; Beaudoin, E.; Maria, S.; Phan, T. N. T.; Gigmes, D.; Giroud, E.; Davidson, P.; Bouchet, R., Comparison of single-ion-conductor block-copolymer electrolytes with Polystyrene-TFSI and Polymethacrylate-TFSI structural blocks. *Electrochim. Acta* **2018,** *269*, 250-261.
67. Bouchet, R.; Maria, S.; Meziane, R.; Aboulaich, A.; Lienafa, L.; Bonnet, J.-P.; Phan, T. N. T.; Bertin, D.; Gigmes, D.; Devaux, D.; Denoyel, R.; Armand, M., Single-ion BAB triblock copolymers as highly efficient electrolytes for lithium-metal batteries. *Nat. Mater.* **2013,** *12*, 452.
68. Porcarelli, L.; Aboudzadeh, M. A.; Rubatat, L.; Nair, J. R.; Shaplov, A. S.; Gerbaldi, C.; Mecerreyes, D., Single-ion triblock copolymer electrolytes based on poly(ethylene oxide) and methacrylic sulfonamide blocks for lithium metal batteries. *J. Power Sources* **2017,** *364*, 191-199.
69. Thelen, J. L.; Inceoglu, S.; Venkatesan, N. R.; Mackay, N. G.; Balsara, N. P., Relationship between Ion Dissociation, Melt Morphology, and Electrochemical Performance of Lithium and Magnesium Single-Ion Conducting Block Copolymers. *Macromolecules* **2016,** *49* (23), 9139-9147.
70. Yu, Y.; Lu, F.; Sun, N.; Wu, A.; Pan, W.; Zheng, L., Single lithium-ion polymer electrolytes based on poly(ionic liquid)s for lithium-ion batteries. *Soft Matter* **2018,** *14*, 6313-6319.
71. Lei, Z.; Wu, P., A highly transparent and ultra-stretchable conductor with stable conductivity during large deformation. *Nat. Commun.* **2019,** *10* (1), 3429.
72. Shi, L.; Zhu, T.; Gao, G.; Zhang, X.; Wei, W.; Liu, W.; Ding, S., Highly stretchable and transparent ionic conducting elastomers. *Nat. Commun.* **2018,** *9* (1), 2630.
73. Zhou, B.; He, D.; Hu, J.; Ye, Y.; Peng, H.; Zhou, X.; Xie, X.; Xue, Z., A flexible, self-healing and highly stretchable polymer electrolyte via quadruple hydrogen bonding for lithium-ion batteries. *J.Mater. Chem. A* **2018,** *6* (25), 11725-11733.
74. Liu, Y.; He, K.; Chen, G.; Leow, W. R.; Chen, X., Nature-Inspired Structural Materials for Flexible Electronic Devices. *Chem. Rev.* **2017,** *117* (20), 12893-12941.
75. Cao, P.-F.; Naguib, M.; Du, Z.; Stacy, E.; Li, B.; Hong, T.; Xing, K.; Voylov, D. N.; Li, J.; Wood, D. L.; Sokolov, A. P.; Nanda, J.; Saito, T., Effect of Binder Architecture on the Performance of Silicon/Graphite Composite Anodes for Lithium Ion Batteries. *ACS. Appl. Mater. Interfaces* **2018,** *10* (4), 3470-3478.
76. Xing, K.; Tress, M.; Cao, P.; Cheng, S.; Saito, T.; Novikov, V. N.; Sokolov, A. P., Hydrogen-bond strength changes network dynamics in associating telechelic PDMS. *Soft Matter* **2018,** *14* (7), 1235-1246.
77. Wojnarowska, Z.; Knapik, J.; Jacquemin, J.; Berdzinski, S.; Strehmel, V.; Sangoro, J. R.; Paluch, M., Effect of Pressure on Decoupling of Ionic Conductivity from Segmental Dynamics in Polymerized Ionic Liquids. *Macromolecules* **2015,** *48* (23), 8660-8666.
78. Fan, F.; Wang, Y.; Hong, T.; Heres, M. F.; Saito, T.; Sokolov, A. P., Ion Conduction in Polymerized Ionic Liquids with Different Pendant Groups. *Macromolecules* **2015,** *48* (13), 4461-4470.
79. Mangadlao, J. D.; De Leon, A. C. C.; Felipe, M. J. L.; Cao, P.; Advincula, P. A.; Advincula, R. C., Grafted Carbazole-Assisted Electrodeposition of Graphene Oxide. *ACS. Appl. Mater. Interfaces* **2015,** *7* (19), 10266-10274.
80. Boudreault, P.-L. T.; Wakim, S.; Blouin, N.; Simard, M.; Tessier, C.; Tao, Y.; Leclerc, M., Synthesis, Characterization, and Application of Indolo[3,2-b]carbazole Semiconductors. *J. Am. Chem. Soc.* **2007,** *129* (29), 9125-9136.
81. Boudreault, P.-L. T.; Beaupré, S.; Leclerc, M., Polycarbazoles for plastic electronics. *Polymer Chemistry* **2010,** *1* (2), 127-136.
82. Cao, P.-F.; Felipe Mary, J.; Advincula Rigoberto, C., On the Formation and Electropolymerization of a Star Copolymer With Peripheral Carbazoles. *Macromol. Chem. Phys.* **2012,** *214* (3), 386-395.
83. Zhi, Z.; Su, Y.; Xi, Y.; Tian, L.; Xu, M.; Wang, Q.; Padidan, S.; Li, P.; Huang, W., Dual-Functional Polyethylene Glycol-b-polyhexanide Surface Coating with in Vitro and in Vivo Antimicrobial and Antifouling Activities. *ACS. Appl. Mater. Interfaces* **2017,** *9* (12), 10383-10397.
84. Mindemark, J.; Lacey, M. J.; Bowden, T.; Brandell, D., Beyond PEO—Alternative host materials for Li+-conducting solid polymer electrolytes. *Prog. Polym. Sci.* **2018,** *81*, 114-143.
85. Hong, T.; Lai, S.; Mahurin Shannon, M.; Cao, P.-F.; Voylov Dmitry, N.; Meyer Harry, M.; Jacobs Christopher, B.; Carrillo Jan-Michael, Y.; Kisliuk, A.; Ivanov Ilia, N.; Jiang, D.-e.; Long Brian, K.; Mays Jimmy, W.; Sokolov Alexei, P.; Saito, T., Highly Permeable Oligo(ethylene oxide)-co-poly(dimethylsiloxane) Membranes for Carbon Dioxide Separation. *Adv. Sustainable Syst.* **2017,** *2* (4), 1700113.

Elastic Single-ion Conducting Polymer Electrolytes: Towards a Versatile Approach for Intrinsically Stretchable Functional Polymers

Peng-Fei Cao,* [1] Bingrui Li,[2] Guang Yang,[1] Sheng Zhao,[2] Jacob Townsend,[2] Kunyue Xing,[2] Zhe Qiang,[3] Konstantinos D. Vogiatzis,[2] Alexei P. Sokolov,[1,2] Jagjit Nanda,[1] and Tomonori Saito*[1]